Supplementary Information: Spontaneous rolling of a soft sphere on a vertical soft substrate

Surjyasish Mitra[a], A-Reum Kim[b], Boxin Zhao[b,*], and Sushanta K. Mitra [a,**]

[a]Department of Mechanical and Mechantronics Engineering, Waterloo Institute for Nanotechnology, University of Waterloo, 200 University Avenue West, Waterloo, ON N2L 3G1, Canada
[b]Department of Chemical Engineering, Waterloo Institute for Nanotechnology, University of Waterloo, 200 University Avenue West, Waterloo, ON N2L 3G1, Canada

Corresponding authors: *zhaob@uwaterloo.ca, **skmitra@uwaterloo.ca

Within this Supplementary Material, we present additional experimental details like PAAm and PDMS fabrication and characterization, and static and dynamic measurements. We also provide detailed derivation of the torque created due to contact asymmetry.

Fabrication of PAAm

To prepare the elastic spheres, we used acrylamide (AAm) as the monomer, N,N'-Methylene-bis-acrylamide (BIS) as the crosslinker, and 2,4,6-tri-methyl benzoyl-diphenylphosphine oxide (TPO) nanoparticle as the initiator (Step 1, Fig. S1). To prepare the TPO nanoparticles, we dissolved 2.5 wt. % of diphenyl (2,4,6-trimethylbenzoyl) phosphine oxide (M_w = 348.48), 3.75 wt. % of polyvinylpyrrolidone, and 3.75 wt. % of dodecyl surface sodium salt (SDS) in DI water. We then sonnicated the mixture for 5 min at 95°C to obtain 10 wt. % of TPO nanoparticles in DI water. We prepared the pregel solutions by diluting the monomer (4 – 30.0 wt.%), 1 wt.% of the crosslinker (based on the monomer), and 2.5 wt % of TPO nanoparticles (based on the monomer) in 0.5 mM $NaIO_4$ solution, which acts as the oxygen scavenger. Consequently, we suspended 4 μL of the pregel solution in a beaker with n-octane and silicone oil (phenylmethylsiloxane-dimethylsiloxane copolymer, 500 cSt, Gelest), with a 1:2 volumetric ratio between the two to prepare the PAAm spheres. The spherical shapes of the PAAm were obtained by utilizing the density gradient between n-octane (density $\rho = 0.71$ g/cm^3) and the silicone oil ($\rho = 1.08$ g/cm^3). To do so, we poured the heavier silicone oil in a beaker first and then slowly poured octane on top of the oil (Step 2, Fig. S1). A bi-layer solvent with a smooth density gradient was achieved after a wait time of 1 hour (Step 3, Fig. S1). Following that, we pipetted 4 μL of the PAAm pregel solution in the middle of the two solvents (Step 4, Fig. S1) and subsequently cured it under UV light ($\sim$365 nm) for 20 min (Step 5, Fig. S1). We rigorously washed the cured PAAm spheres with heptane before use (Step 6, Fig. S1).

Rheology characterization of PAAm

The elastic properties of the PAAm spheres/drops were characterized using a dynamic shear rheometer (Kinexus Rotational Rheometer, Malvern Instruments). For rheology measurements, each PAAm was polymerized in a petri dish with a thickness of 2 mm. The shear storage (G') and loss (G'') modulus of the materials were measured by performing a frequency sweep test on the rheometer from 0.01 to 100 Hz at a strain rate of 1 % and a normal force of 1 N (Fig. S2). All measurements were performed at 25°C, using a parallel plate geometry with a 25 mm diameter plate as the test adopter. The measurements are taken after waiting for 10 min to stabilize the polymer. From the measured G' and G'' values, we calculated the absolute shear modulus $|G| = \sqrt{G'^2 + G''^2}$. Consequently, we used the absolute modulus G at the lowest frequency $f = 0.01$ Hz to obtain the static shear modulus $G_{0,1}$. The elastic modulus is subsequently calculated using the relation $E_1 = 3G_{0,1}$, i.e., considering the Poisson's ratio $\nu = 1/2$ [1].

Fabrication and characterization of soft substrates

Soft substrates were prepared using two different commercially available polydimethylsiloxane: PDMS, Sylgard 184 and PDMS, Sylgard 527. First, the base and curing agent of Sylgard 184 and 527 were mixed in the manufacturer specified weight ratios of 10:1 and 1:1, respectively. The mixture was then thoroughly stirred, dessicated to remove trapped bubbles, and finally cured at 85°C for 12 hours. Before use, the cured substrates were kept at room temperature for 2 hours. Using this technique, we prepared soft coatings of 1 mm thickness on underlying glass substrates. The shear storage and loss modulus of the soft materials were measured by performing a frequency sweep test on a dynamic shear rheometer (Kinexus Rotational Rheometer, Malvern Instruments) from 0.01 to 100 Hz at a strain rate of 1 % and a normal force of 1 N (Fig. S3). Here also, from the measured G' and G'' values, we calculated the absolute shear modulus $|G| = \sqrt{G'^2 + G''^2}$. Consequently, we used the absolute modulus G at the lowest frequency $f = 0.01$ Hz to obtain the static shear modulus $G_{0,2}$. The elastic modulus is subsequently calculated using the relation $E_2 = 3G_{0,2}$, i.e., considering the Poisson's ratio $\nu = 1/2$. Additionally, we performed atomic force microscopy measurements (Nanoscope, Digital Instruments) on the Sylgard 184, 10:1 PDMS, i.e., the soft substrate on which rolling was observed. Representative AFM measurements are shown in Fig. S8. On average, the arithmetic mean roughness (R_a) and the root mean square height (R_q) are 0.76 ± 0.06 nm and 0.95 ± 0.08 nm, respectively.

Derivation of pressure distribution and torque across the contact interface

We assume two elastic surfaces (say, spheres) with elasticity E_1 and E_2, and with characteristic length scale R. The general pressure distribution for symmetric contact of these two elastic surfaces can be expressed as the superposition of the Hertz problem and the Bousinessq problem [2]:

$$p(r, a, \delta) = p_\mathrm{H}\left(1 - \frac{r^2}{a^2}\right)^{1/2} + p_\mathrm{B}\left(1 - \frac{r^2}{a^2}\right)^{-1/2} \tag{1}$$

Here, a and δ are the contact radius and indentation depth, respectively. For Hertz [3] or JKR [4] type contacts (Fig. S9a) with symmetric pressure distribution, we have $p_\mathrm{H} = \frac{2aE^*}{\pi R}$ and $p_\mathrm{B} = -\frac{2E^*\delta}{\pi a}$. By the virtue of symmetry, we have $p(x, y) = -p(x, y)$ and thus there is no rolling moment about the y-axis (Fig. S9a) since $M_y = \int\int xp(x, y)dxdy = 0$ [2]. For asymmetric contact, we now have to unequal radii a_1 and a_2 where $a_1 > a_2$ (Fig. S9b). Unequal contact radii thus changes the Boussinesq part of the solution as,

$$p_\mathrm{B}(a) = \frac{E^*}{\pi a}\delta - \frac{1}{2}p_\mathrm{H}(a), \tag{2}$$

where the Hertz part of the solution $p_\mathrm{H}(a) = \frac{2aE^*}{\pi R}$ remains unchanged. Thus, the modified general pressure distribution for asymmetric contact can be expressed as ,

$$p(r, a, \delta) = p_\mathrm{H}(a)\left(1 - \frac{r^2}{a^2}\right)^{1/2} + \left(\frac{E^*}{\pi a}\delta - \frac{1}{2}p_\mathrm{H}(a)\right)\left(1 - \frac{r^2}{a^2}\right)^{-1/2} \tag{3}$$

However, the pressure distribution is different in the two halves of the contact (Fig. S9b) and can be expressed as [2],

$$p(r, a, \delta) = p(r, a_1, \delta), x < 0 \tag{4}$$

$$p(r, a, \delta) = p(r, a_2, \delta), x > 0 \tag{5}$$

The pressure difference due to the two unequal halves generates a moment about the y-axis as [2],

$$M_\mathrm{y} = \int_{\pi/2}^{3\pi/2}\int_0^{a_1} xp(r, a_1, \delta)rdrd\phi + \int_{-\pi/2}^{\pi/2}\int_0^{a_2} xp(r, a_2, \delta)rdrd\phi \tag{6}$$

where $x = r\cos\phi$ and $y = r\sin\phi$. Consequently, the moment can be expressed as,

$$M_{\rm y} = -2\int_0^{a_1} r^2 p(r, a_1, \delta)dr + 2\int_0^{a_2} r^2 p(r, a_2, \delta)dr \tag{7}$$

$$= -2\int_0^{a_1} r^2 \left[p_{\rm H}(a_1)\left(1 - \frac{r^2}{{a_1}^2}\right)^{1/2} + \left(\frac{E^*}{\pi a_1}\delta - \frac{1}{2}p_{\rm H}(a_1)\right)\left(1 - \frac{r^2}{{a_1}^2}\right)^{-1/2}\right] dr \tag{8}$$

$$+ 2\int_0^{a_2} r^2 \left[p_{\rm H}(a_2)\left(1 - \frac{r^2}{{a_2}^2}\right)^{1/2} + \left(\frac{E^*}{\pi a_2}\delta - \frac{1}{2}p_{\rm H}(a_2)\right)\left(1 - \frac{r^2}{{a_2}^2}\right)^{-1/2}\right] dr \tag{9}$$

$$= -2\int_0^{a_1} r^2 \left[\frac{2a_1E^*}{\pi R}\left(1 - \frac{r^2}{{a_1}^2}\right)^{1/2} + \left(\frac{E^*}{\pi a_1}\delta - \frac{1}{2}\frac{2a_1E^*}{\pi R}\right)\left(1 - \frac{r^2}{{a_1}^2}\right)^{-1/2}\right] dr \tag{10}$$

$$+ 2\int_0^{a_2} r^2 \left[\frac{2a_2E^*}{\pi R}\left(1 - \frac{r^2}{{a_2}^2}\right)^{1/2} + \left(\frac{E^*}{\pi a_2}\delta - \frac{1}{2}\frac{2a_2E^*}{\pi R}\right)\left(1 - \frac{r^2}{{a_2}^2}\right)^{-1/2}\right] dr \tag{11}$$

$$= -\frac{\pi {a_1}^3}{4}\left(\frac{2E^*\delta}{\pi a_1} - \frac{a_1E^*}{\pi R}\right) + \frac{\pi {a_2}^3}{4}\left(\frac{2E^*\delta}{\pi a_2} - \frac{a_2E^*}{\pi R}\right) \tag{12}$$

$$= \frac{{a_1}^2E^*}{4R}({a_1}^2 - 2\delta R) - \frac{{a_2}^2E^*}{4R}({a_2}^2 - 2\delta R) \tag{13}$$

$$= \frac{E^*}{4R}\left[({a_1}^2 - \delta R)^2 - ({a_2}^2 - \delta R)^2\right] \tag{14}$$

$$= \frac{\pi R}{2}(a_1G_1 - a_2G_2) \tag{15}$$

where, $G_1 = \frac{E^*}{2\pi}\frac{({a_1}^2 - \delta R)^2}{a_1 R}$ and $G_2 = \frac{E^*}{2\pi}\frac{({a_2}^2 - \delta R)^2}{a_2 R}$ are the strain energy release rates at the receding and advancing edge, respectively.

Description of supplementary videos

- **Supplementary movie S1**: Glass sphere falling off. Fall-off of a 1 mm radius glass sphere from a vertial glass substrate. Image acquisition rate is 1000 frames per second and spatial resolution is 7-8 μm/pixel.
- **Supplementary movie S2**: Sliding water droplet. Sliding of a 1 mm radius water droplet on a vertical glass substrate. Image acquisition rate is 10 frames per second and spatial resolution is 25 μm/pixel.
- **Supplementary movie S3**: Rolling on a 90° degree incline: Run1. Rolling of a 1 mm radius PAAm 30 wt.% elastic sphere (elasticity, $E_1 = 169.7$ kPa) on a vertical PDMS substrate (elasticity, $E_2 = 2242$ kPa). Image acquisition rate is 50 frames per second and spatial resolution is 7-8 μm/pixel.
- **Supplementary movie S4**: Rolling on a 90° degree incline: Run2. Rolling of a 1 mm radius PAAm 30 wt.% elastic sphere (elasticity, $E_1 = 169.7$ kPa) on a vertical PDMS substrate (elasticity, $E_2 = 2242$ kPa). Image acquisition rate is 50 frames per second and spatial resolution is 7-8 μm/pixel.
- **Supplementary movie S5**: Rolling on a 90° degree incline: Run3. Rolling of a 1 mm radius PAAm 30 wt.% elastic sphere (elasticity, $E_1 = 169.7$ kPa) on a vertical PDMS substrate (elasticity, $E_2 = 2242$ kPa). Image acquisition rate is 60 frames per second and spatial resolution is 7-8 μm/pixel.
- **Supplementary movie S6**: Rolling with microplastics. Rolling of a 1 mm radius PAAm 30 wt.% elastic sphere (elasticity, $E_1 = 169.7$ kPa) on a vertical PDMS substrate (elasticity, $E_2 = 2242$ kPa) with microplastics dispersed on the substrate. Image acquisition rate is 60 frames per second and spatial resolution is 7-8 μm/pixel.
- **Supplementary movie S7**: Crack opening and closing. Rolling of a 1 mm radius PAAm 30 wt.% elastic sphere (elasticity, $E_1 = 169.7$ kPa) on a vertical PDMS substrate (elasticity, $E_2 = 2242$ kPa)

highlighting the crack opening and closing. Image acquisition rate is 60 frames per second and spatial resolution is 2 μm/pixel.

- **Supplementary movie S8**: Rolling and stopping. Rolling of a 1 mm radius PAAm 30 wt.% elastic sphere (elasticity, $E_1 = 169.7$ kPa) on a vertical PDMS substrate (elasticity, $E_2 = 2242$ kPa). Image acquisition rate is 10 frames per second and spatial resolution is 22 μm/pixel.
- **Supplementary movie S9**: Extended rolling. Rolling of a 1 mm radius PAAm 30 wt.% elastic sphere (elasticity, $E_1 = 169.7$ kPa) on a vertical PDMS substrate (elasticity, $E_2 = 2242$ kPa). Image acquisition rate is 10 frames per second and spatial resolution is 22 μm/pixel.

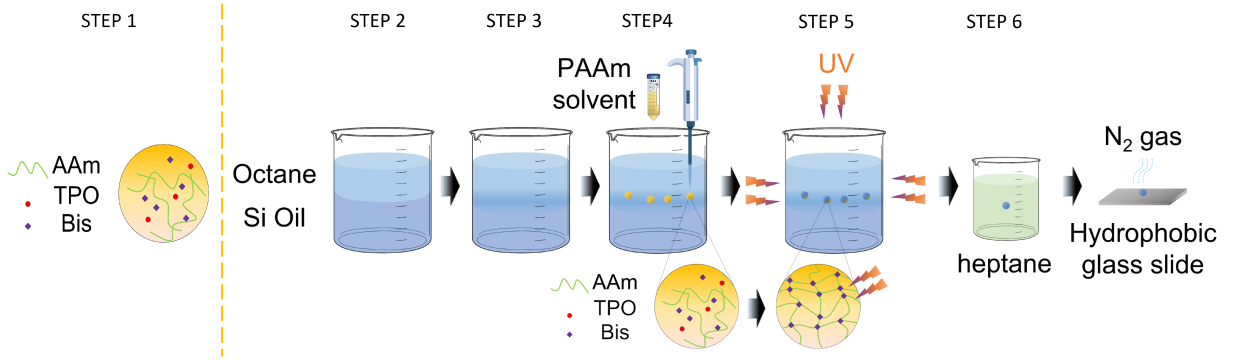

FIG. S1. Schematic showing the different steps of the PAAm elastic spheres/drops preparation procedure. Here, AAm: Acrylamide, TPO: 2,4,6-tri-methyl benzoyldiphenylphosphine oxide, and Bis: N,N'-Methylene-bis-acrylamide. Adapted with permission from Ref. [5].

[1] A.-R. Kim, S. Mitra, S. Shyam, B. Zhao, and S. K. Mitra, Flexible hydrogels connecting adhesion and wetting, Soft Matter **20**, 5516 (2024).

[2] C. Dominik and A. Tielens, Resistance to rolling in the adhesive contact of two elastic spheres, Phil. Mag. A **72**, 783 (1995).

[3] H. Hertz, Über die berührung fester elastischer körper, J. für die reine und Angew. Math. **92**, 22 (1882).

[4] K. L. Johnson, K. Kendall, and A. D. Roberts, Surface energy and the contact of elastic solids, Proc. Royal Soc. Lon. A. **324**, 301 (1971).

[5] S. Mitra, A.-R. Kim, B. Zhao, and S. K. Mitra, Rapid spreading of yield-stress liquids, Langmuir **40**, 18968 (2024).

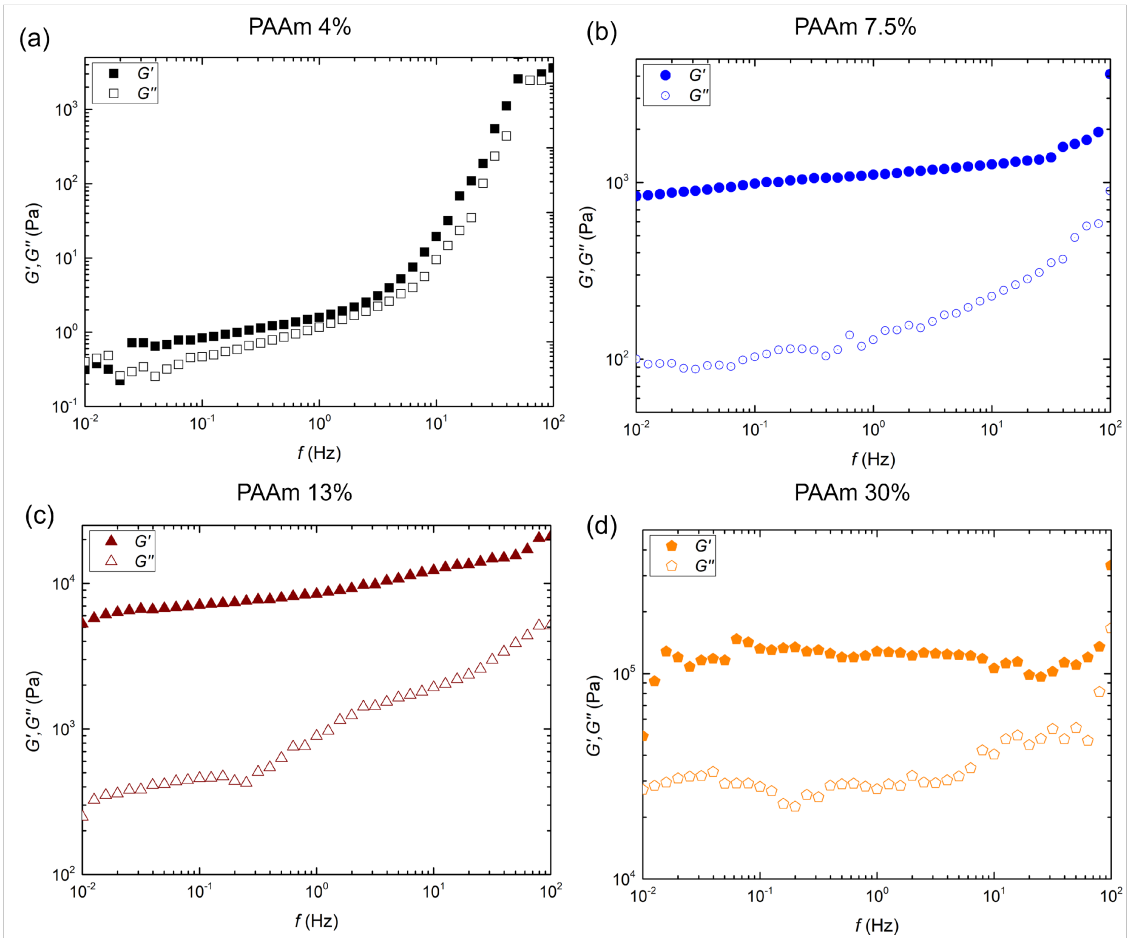

FIG. S2. Variation of shear storage modulus (G') and shear loss modulus (G'') with frequency f for (a) PAAm with 4 wt.% monomer, (b) PAAm with 7.5 wt.% monomer, (c) PAAm with 13 wt.% monomer, and (d) PAAm with 30 wt.% monomer. Subfigure (d) adapted with permission from Ref. [1].

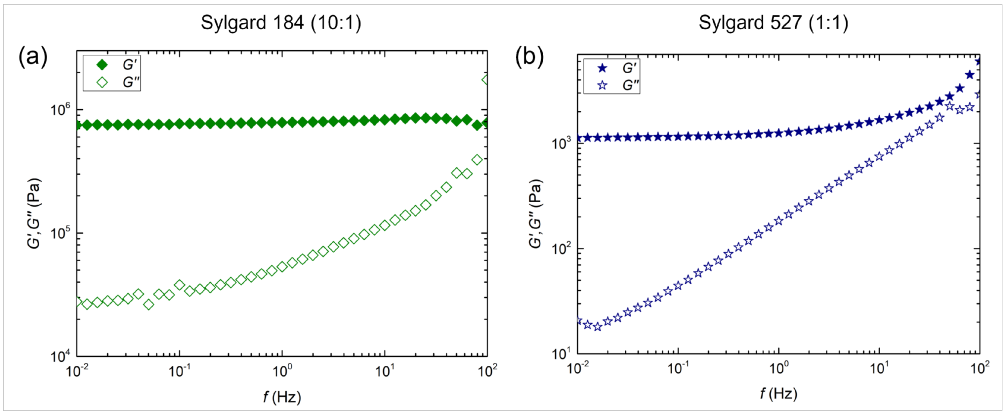

FIG. S3. Variation of shear storage modulus (G') and shear loss modulus (G'') with frequency f for (a) PDMS, Sylgard (10:1) and (b) PDMS, Sylgard 527 (1:1).

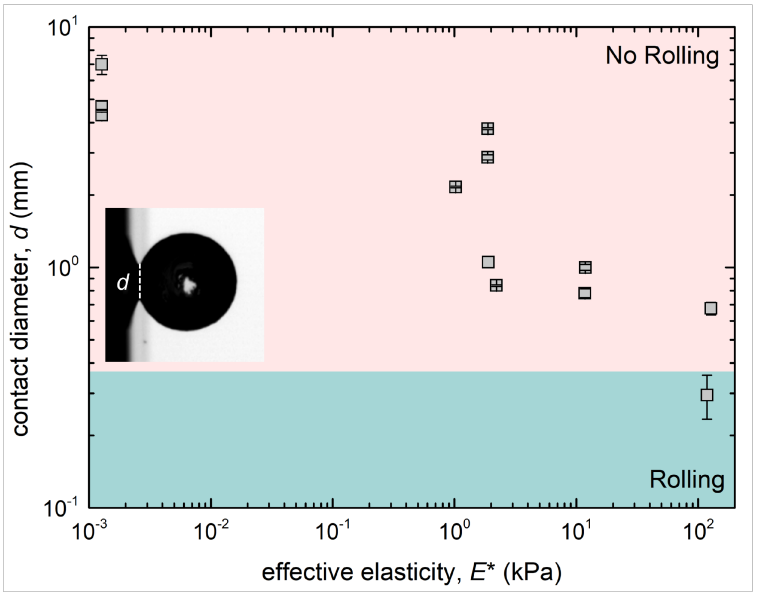

FIG. S4. Variation of contact diameter d with effective elasticity E^* for contact of PAAm spheres/drops (elasticity, E_1) on soft PDMS substrates (elasticity, E_2). The contact diameter for the rolling event is calculated by averaging over several frames of multiple rolling experiments. Inset shows a representative experimental snapshot highlight the contact diameter d.

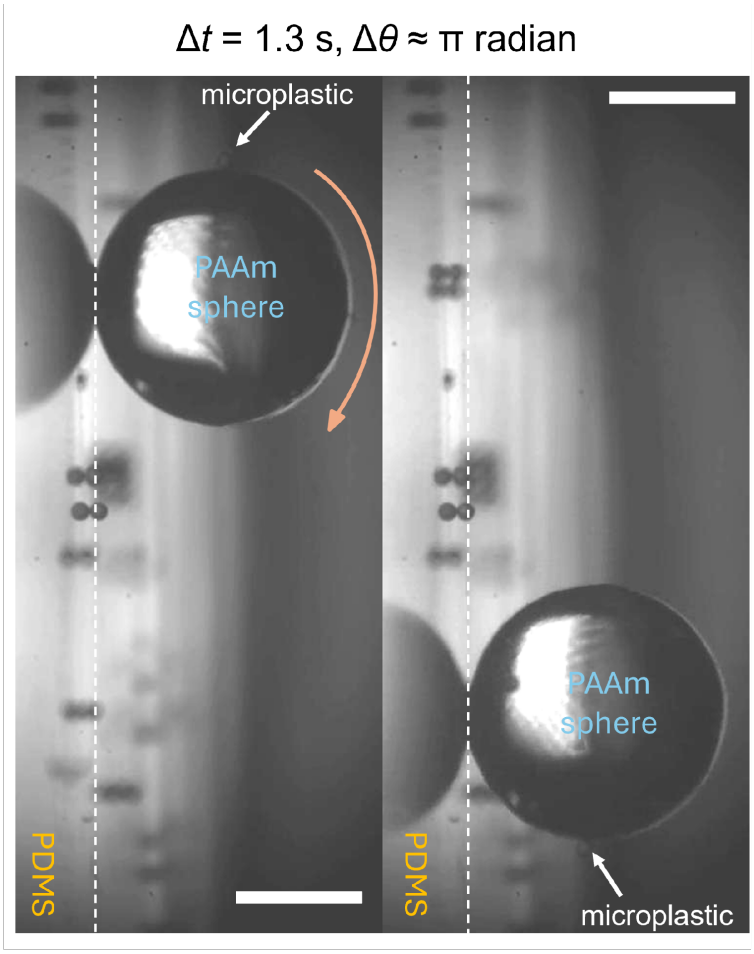

FIG. S5. Experimental snapshots of a rolling event where microplastics are randomly dispersed along the path of the rolling PAAm sphere (elasticity, $E_1 = 169.7$ kPa) on PDMS (elasticity, $E_2 = 2422$ kPa) substrates. The rolling sphere picks one up along the way which rotates with the sphere. The time interval between the snapshots $\Delta t = 1.3\,\mathrm{s}$ during which the microplastic has undergone rotation of $\Delta\theta \approx \pi$ radians leading to angular velocity, $\omega = \Delta\theta/\Delta t = 2.4\,\mathrm{rad/s}$. Scale bar represents 1 mm.

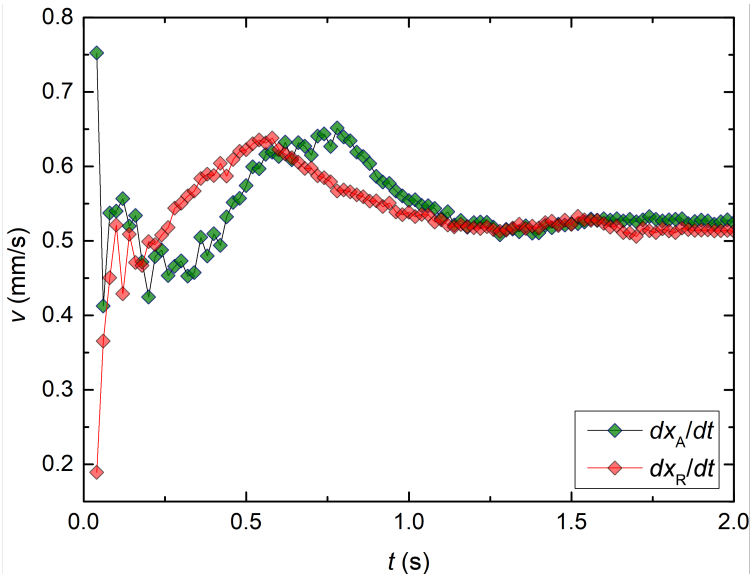

FIG. S6. Evolution of instantaneous velocity v calculated using finite difference of the advancing ($dx_{\rm A}/dt$) and receding ($dx_{\rm R}/dt$) edges during rolling of a PAAm sphere (elasticity, $E_1 = 169.7$ kPa) on a PDMS substrate (elasticity, $E_2 = 3$ kPa).

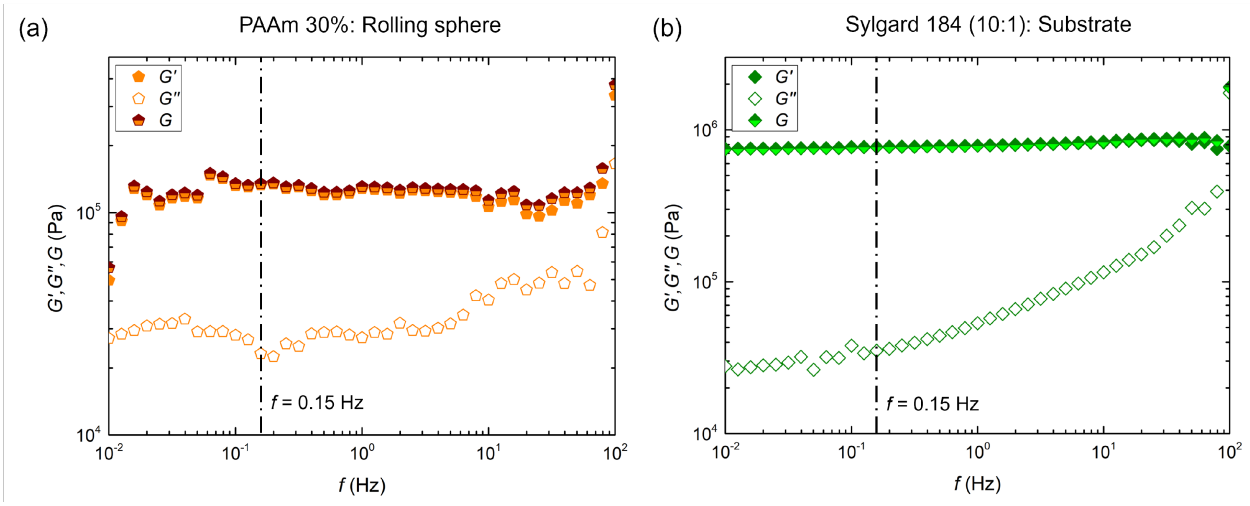

FIG. S7. Variation of shear storage modulus (G') and shear loss modulus (G''), and absolute shear modulus $|G| = \sqrt{G'^2 + G''^2}$ with frequency f for (a) PAAm with 30 wt.% monomer and (b) PDMS, Sylgard (10:1). The dot-dashed lines show the frequency, i.e., $f = 0.15$ Hz at which effective elasticity is considered.

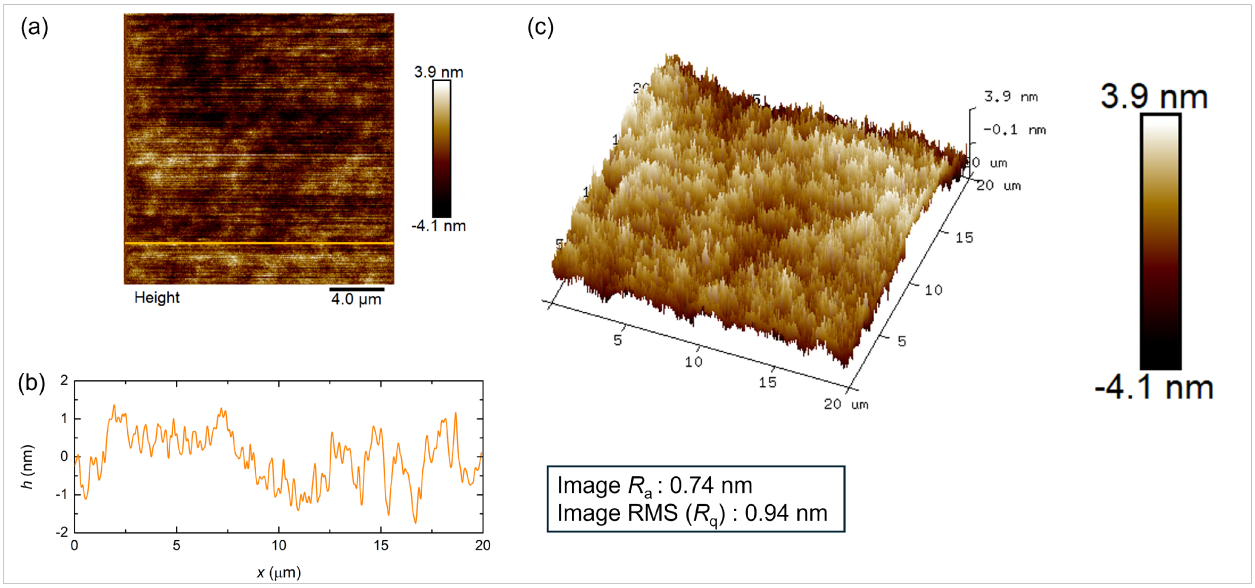

FIG. S8. a) Atomic force microscopy (AFM) scan on a 20 μm x 20 μm cross-section of a Sylgard 184 10:1 PDMS substrate with elastic modulus, $E_2 = 2422$ kPa, i.e., the substrate upon which rolling is observed. (b) Surface profile obtained along the orange line shown in (a). (c) Three-dimensional profile of the entire scan shown in (a). R_a and R_q values for the scan are shown.

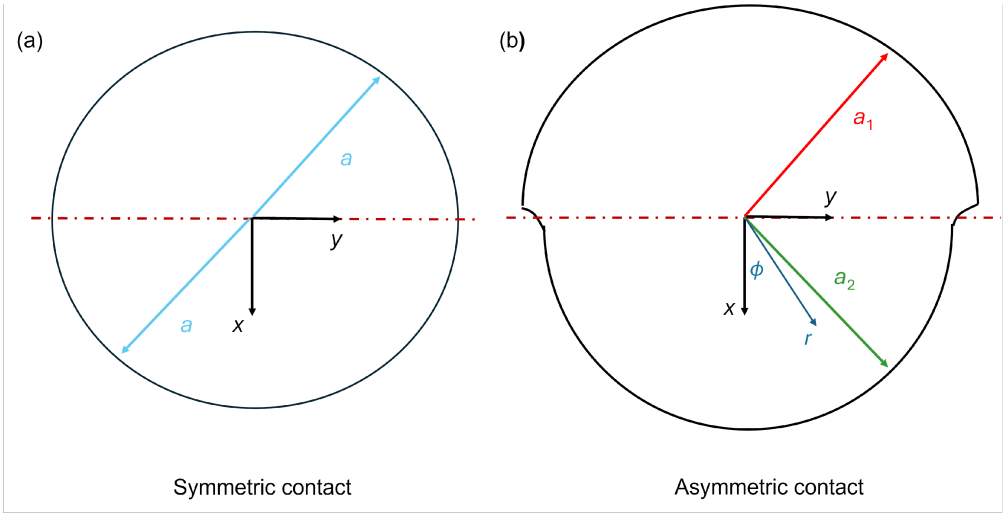

FIG. S9. Bottom-view schematic highlighting (a) symmetric and (b) asymmetric contact configurations. a is the contact radius for symmetric contact whereas a_1 and a_2 are the contact radii for asymmetric contact. r and ϕ are the radial and angular coordinates.